Pre-Clinical Research Report

Journal of INTERNATIONAL MEDICAL RESEARCH

Journal of International Medical Research
2019, Vol. 47(3) 1250–1263

DOI: 10.1177/0300060518813058
journals.sagepub.com/home/imr
SAGE

Protective role of arnebin-1 in rats with nonalcoholic fatty liver disease

Weijia Yang, Minchun Yang, Hui Yao, Yelin Ma, Xuanxuan Ren, Long Teng and Tao Wang

Abstract

Objective: To examine the effects of arnebin-1 on nonalcoholic fatty liver disease (NAFLD) induced by a high-fat diet (HFD).

Methods: Male Sprague–Dawley rats were fed an HFD for 10 weeks and then treated with arnebin-1 at a dose of 5, 10 or 20 mg/kg/day by gavage for a further 12 weeks of a 22-week HFD. Peripheral blood and liver tissues were collected for biochemical and histopathological examination. The mechanisms of arnebin-1 on liver fibrosis and insulin resistance (IR) were determined by Western blotting and real-time quantitative polymerase chain reaction.

Results: Arnebin-1 treatment attenuated the increase of total cholesterol, triglycerides, low-density lipoprotein cholesterol, aspartate aminotransferase and alanine aminotransferase in serum and lipid accumulation in the livers of HFD-fed rats. Furthermore, arnebin-1 abrogated HFD-induced liver fibrosis and the increase of fibrotic biomarkers. The HFD-induced decrease of hepatic proliferator-activated receptor γ and pro-matrix-metalloproteinase (MMP)-9 levels and the increase of tissue inhibitor of metalloproteinase-1 (TIMP-1) levels were reversed after arnebin-1. Arnebin-1 attenuated IR through activating the insulin receptor substrate-1/Akt/mTOR signalling pathway.

Conclusion: This study demonstrated that arnebin-1 ameliorates NAFLD, in part, by attenuating hepatic fibrosis and IR, suggesting that arnebin-1 may be a therapeutic agent for NAFLD treatment.

Keywords

Nonalcoholic fatty liver disease, lipid accumulation, liver injury, fibrosis, insulin resistance, arnebin-1

Date received: 5 July 2018; accepted: 19 October 2018

Introduction

Nonalcoholic fatty liver disease (NAFLD) is the most common form of liver disease and is considered to be the hepatic manifestation of metabolic syndrome.[1,2] Clinical research has

Department of Internal Medicine of Traditional Chinese Medicine, Zhejiang Hospital, Hangzhou, Zhejiang Province, China

Corresponding author:
Minchun Yang, Department of Internal Medicine of Traditional Chinese Medicine, Zhejiang Hospital, 12 Lingyin Road, Xihu District, Hangzhou, Zhejiang, 310013, China.
Email: yangmc_zjh@163.com

demonstrated that NAFLD develops from simple steatosis to nonalcoholic steatohepatitis (NASH), fibrosis, cirrhosis and even hepatocellular carcinoma.[3–6] Approximately 10–29% of patients with NASH will develop cirrhosis and liver cancer within a 10-year period.[2] Furthermore, previous studies indicate that NASH and NAFLD are associated with an increased risk of cardiovascular disease.[6,7] Although some health interventions (e.g. exercise and dietary regulation) and medicines (e.g. fibrate, statins and metformin) have been suggested to delay the progress of NAFLD, there remains a lack of effective strategies or approaches.[7,8] Thus, it is extremely important to identify effective regimens for NAFLD treatment.

Zicao, a traditional Chinese herbal plant, belongs to the Boraginaceae family of perennial herbs and has been widely used for many years for the treatment of burns, carbuncles, measles, macular eruptions and sore throats.[9,10] Arnebin-1 is one of the main natural naphthoquinone derivatives of Zicao.[11–13] *In vivo* and *in vitro* experimental models have demonstrated that arnebin-1 exerts antihyperglycaemic activity and accelerates wound healing through the phosphatidylinositol-3-kinase-dependent pathway.[11,12] Notably, previous studies showed that another naphthoquinone derivative of Zicao, acetylarnebin-1, effectively ameliorated rat obesity induced by a high-fat diet (HFD) by attenuating lipid dysregulation and inflammation.[13,14] These findings suggest that Zicao may be beneficial for NAFLD treatment. The present study investigated the potential therapeutic effects of arnebin-1 on hepatic lipid dysregulation and injury in a rat model of HFD-induced NAFLD.

Materials and methods

Materials

Arnebin-1 (purity > 98%) was obtained from Wuhan Tianzhi Biotechnology (Wuhan, China) and dissolved in 0.1 mM phosphate-buffered saline (pH 7.4). Kits for determining serum total cholesterol (TC), triglycerides (TG), high-density lipoprotein cholesterol (HDL-C), low-density lipoprotein cholesterol (LDL-C), aspartate aminotransferase (AST) and alanine aminotransferase (ALT) were purchased from Jiancheng Biological Engineering Institute (Nanjing, China). Antibodies against proliferator-activated receptor γ (PPARγ), matrix-metalloproteinase-9 (MMP-9), tissue inhibitor of metalloproteinase-1 (TIMP-1), p-Akt (Ser473), Akt, p-mTOR (Ser2448), mTOR, glyceraldehyde 3-phosphate dehydrogenase (GAPDH) and horseradish peroxidase (HRP)-conjugated secondary antibodies were purchased from Santa Cruz Biotechnology Inc. (Santa Cruz, CA, USA). Rat TIMP-1 enzyme-linked immunosorbent assay (ELISA) kit, p-insulin receptor substrate (IRS)-1 (Tyr608/612), p-IRS-1 (Ser307) and IRS-1 were obtained from Abcam® (Cambridge, MA, USA). A rat total MMP-9 ELISA Kit was obtained from R&D Systems (Minneapolis, MN, USA).

Animals

Fifty male Sprague–Dawley rats (8-weeks old; 200–250 g) were obtained from The Jackson Laboratory (Sacramento, CA, USA) and were housed under a 12-h light/12-h dark cycle with free access to food and water. All rats were randomized into five groups ($n = 10$ per group) according to a computer-generated randomization schedule: normal control group (control), HFD group (NAFLD), low-dose arnebin-1 treatment group (ANB-L), medium-dose arnebin-1 treatment group (ANB-M) and high-dose arnebin-1 treatment group (ANB-H). The rats in the control group were fed with a standard diet and the other four groups were fed with an HFD (45% kcal fat; D12451; Research Diets,

New Brunswick, NJ, USA). 10 weeks later, the rats in the ANB-L, ANB-M and ANB-H groups were intragastrically administrated arnebin-1 at a dose of 5, 10 or 20 mg/kg/day in 0.5 ml volume for another 12 weeks (a total of 22 weeks of an HFD), respectively. In the control HFD group (NAFLD group), rats were intragastrically administrated 0.1 ml/100 g physiological saline for 12 weeks. Rats in the normal control group (control) were fed a standard diet and were not given any treatment. To investigate the effect of arnebin-1 on the hepatic insulin signalling pathway *in vivo*, the rats were injected intraperitoneally with insulin (1.0 IU/kg for 15 min) after arnebin-1 treatment for 12 weeks (a total of 22 weeks of an HFD). The changes to the insulin signalling pathway were determined by investigating IRS-1 phosphorylation at Tyr608, Akt phosphorylation at Ser473, mTOR phosphorylation at Ser2448 and IRS-1 phosphorylation at Ser307 using Western blotting.

Animal experiments were approved by the Committee on the Ethics of Animal Experiments of Zhejiang Hospital, Hangzhou, Zhejiang Province, China and were performed according to the guidelines for the ethical care of animals (approval no. SYXK 2016-0014).

Determination of blood biochemistry

Blood samples (approximately 0.8 ml) was collected from the abdominal vena cava at the end of the experimental period using heparin lithium-anticoagulant tubes. Rats were fasted for 10 h before blood glucose and plasma insulin measurements. Blood glucose was measured using commercial test strips (OneTouch® Ultra® Blood Glucose Monitoring System; Lifescan, Burnaby, BC, Canada). The level of insulin in plasma was determined using an insulin ELISA kit (Crystal Chem, Elk Grove Village, IL, USA) according to the manufacturer's protocol. For serum TC, TG, HDL-C, LDL-C, AST, ALT, MMP-9 and TIMP-1 levels determination, whole blood was centrifuged at 3000 *g* for 10 min at room temperature to obtain serum (Allegra® 64R benchtop centrifuge; Beckman Coulter, Brea, CA, USA). The above indices were examined using commercially available kits according to the manufacturers' instructions. The homeostasis model assessment of insulin resistance (HOMA-IR) index was calculated as follows: fasting blood glucose × fasting insulin/22.5. A glucose tolerance test (GTT) and insulin tolerance test (ITT) were performed in rats after they had received the 22-week HFD. GTT was monitored in 10-h fasted rats followed by an intraperitoneal injection of glucose 1.5 g/kg, while ITT was performed in non-fasted rats after an intraperitoneal injection of insulin 0.5 IU/kg.

Histopathological examination

Following the 12-week treatment with arnebin-1, rats were sacrificed and the livers were subjected to routine histopathological examination. Liver samples were fixed in 30% formalin, dehydrated in ethanol and embedded in paraffin. All specimens were sliced continuously into 5-μm-thick sections and stained with haematoxylin and eosin, oil Red O or Masson's trichrome stain. All slides were analysed under a CKX41 optical microscope (Olympus Optical, Tokyo, Japan).

Determination of biochemistry in liver tissues

At the end of the experiment, rat livers were harvested. Liver homogenates were prepared in anhydrous alcohol using a homogenizer (PK-01200UHD; Grainger, Miami, FL, USA) and centrifuged at 12000 *g* for 15 min at 4°C (Allegra® 64R benchtop centrifuge; Beckman Coulter). The supernatant was collected for TC, TG, MMP-9 and TIMP-1

determination according to the same protocol that was used for the blood biochemistry measurements. Hepatic TC and TG levels were normalized to the amount of total protein of each liver sample as determined using an Enhanced BCA Protein Assay Kit (Beyotime, Jiangsu, China).

Western blot analyses

Equal amounts of protein (50 μg) were separated by 8–10% sodium dodecyl sulphate–polyacrylamide gel electrophoresis (SDS–PAGE) (Mini-PROTEAN® Tetra Cell System; BioRad, Hercules, CA, USA) and then transferred to polyvinylidenefluoride (PVDF) membranes (Millipore, Billerica, MA, USA). The PVDF membranes were blocked in 5% skimmed milk in Tris-buffered saline Tween-20 (TBST; 10 mM Tris-HCl, 150 mM NaCl, 0.05% Tween-20, pH 7.6) for 1 h and subsequently treated with the appropriate antibodies against the following proteins at 4°C overnight: PPARγ, MMP-9, TIMP-1 and β-actin (dilution 1:1000 for each). The membranes were washed with TBST three times and then incubated with the appropriate HRP-conjugated secondary antibodies (dilution 1:2000) for 1 h at room temperature. After washing with TBST three times, the signals were determined using an enhanced chemiluminescence kit (Beyotime) and the intensity of the protein bands was analysed using ImageJ software version 1.4.[15]

Real-time quantitative PCR

Total RNA (1 μg) was isolated from liver tissues using TRIzol® reagent (Invitrogen, Carlsbad, CA, USA) according to the manufacturer's instructions. Complimentary DNA was synthesized through reverse transcription of RNA using the SuperScript™ III First-Strand Synthesis System (Invitrogen). The polymerase chain reaction (PCR) amplifications were performed using Applied Biosystems™ Fast SYBR™ Green Master Mix (Applied Biosystems, Foster City, CA, USA) with an Applied Biosystems™ Prism 7300 Fast Real-Time PCR system (Applied Biosystems). The specific primer sequences were synthesized and provided by Shengong Co. Ltd. (Shanghai, China): plasminogen activator inhibitor type 1 (PAI-1), sense 5′-AGCTTTGTGAAGGAGGACC G-3′ and antisense 5′-CAGGGATGC AGACCCCAAAT-3′; connective tissue growth factor (CTGF), sense 5′-GCCCG CCTAG TCTCACAC-3′ and antisense 5′-GTCACGCTCC GTACACAGTT-3′; collagen III, sense 5′-ACGTAAGCACTGGT GGACAG-3′ and antisense 5′-GGAGGG CCATAGCTGAACTG-3′; collagen IV, sense 5′-GGGGTCGGGCTGGGAGTG AT-3′ and antisense 5′-GCTGGCCGTCC ATACCCGTG-3′; PPARγ, sense 5′-GAG GATCCCCGGGGTACCGGATGACCA TGGTTGACACAG-3′ and antisense 5′-A CATTCCACAGTTAGCTAGCTAAGCA TAGTC TGGGACATCATAAGGGTA-3′; MMP-9, sense 5′-TTTGACAGCGACAA GAAGTGG-3′ and antisense 5′-TCCC ATCCTTGAACAAATACA-3′; TIMP-1, sense 5′-CCTTCTGCAATTCCGACCTC-3′ and antisense 5′-CGGGCAGGATTC AGG CTAT-3′; and GAPDH, sense 5′-GCCAT CGTCACC AACTGGGAC-3′ and antisense 5′-CGATTTCCCGCTCGGCCGTG G-3′. The cycling programme involved preliminary denaturation at 95°C for 1 min, followed by 40 cycles of denaturation at 95°C for 15 s, annealing at 60°C for 30 s, and elongation at 72°C for 30 s, followed by a final elongation step at 72°C for 10 min. Target gene expression ($2^{-\Delta\Delta Ct}$) was normalized to endogenous GAPDH expression.

Zymographic analysis for MMP-9/NGAL and MMP-9 gelatinolytic activities

The gelatinolytic activities of MMP-9/neutrophil gelatinase-associated lipocalin

(NGAL) and MMP-9 in liver tissues were determined by zymography as described previously with some modifications.[16] Aliquots of protein (20 μg) were subjected to SDS–PAGE with 1% gelatin as a substrate under nonreducing conditions. Following electrophoresis, the gels were washed with 2.5% Triton X-100 twice for 1 h and then incubated in 50 mmol/l Tris-HCl buffer (pH 7.4) overnight at room temperature. Afterwards, the gels were stained with Coomassie Brilliant Blue R-250 (Merck, Darmstadt, Germany) for 1 h and washed with deionized water. Clear bands within the gel indicated the areas of proteolysis against a blue background. MMP-9/NGAL and pro-MMP-9 were determined in accordance with pre-stained protein standards (BioRad) co-electrophoresed in these gels. The gelatinolytic activities of MMP-9/NGAL and MMP-9 were analysed using ImageJ software version 1.4.[15]

Cell culture

HepG2 cells (American Type Culture Collection, Manassas, VA, USA) were cultured in Dulbecco's Modified Eagle's Medium supplemented with 10% heat-inactivated fetal bovine serum and 1% penicillin/streptomycin (all from GIBCO® Cell Culture, Carlsbad, CA, USA) at 37°C in a 95:5 air/CO_2 humidified atmosphere.

Statistical analyses

All statistical analyses were performed using the SPSS® statistical package, version 19.0 (IBM Corp, Armonk, NY, USA). All parameters are expressed as mean ± SD. The results were statistically analysed using one-way analysis of variance followed by Tukey's multiple comparison test. A P-value < 0.05 was considered statistically significant.

Results

At the end of the experimental treatment, the HFD-treated rats (NAFLD group) had reached a significantly higher body weight than the control rats ($P < 0.05$), which was significantly decreased by arnebin-1 treatment in a dose-dependent manner ($P < 0.05$ for all comparisons compared with the NAFLD group) (Table 1). Administration of arnebin-1 significantly decreased the levels of serum ALT and AST in HFD-fed rats compared with the NAFLD group ($P < 0.05$ for all comparisons). To investigate the effect of arnebin-1 on lipid profiles, the serum TC, TG,

Table 1. Body weight and biochemical parameters in control and experimental groups of Sprague–Dawley rats after 10 weeks of either a standard diet (control group) or a high-fat diet followed by 12 weeks of treatment with either saline (NAFLD group) or arnebin-1 in addition to the existing diet.

	Groups of Sprague–Dawley rats				
Parameters	Control	NAFLD	ANB-L	ANB-M	ANB-H
Body weight, g	348.7 ± 6.6	431.8 ± 10.1*	403.6 ± 9.6#	371.3 ± 10.7#	357.4 ± 9.9#
ALT, IU/l	27.10 ± 3.20	89.80 ± 5.42*	76.50 ± 4.10#	61.20 ± 3.20#	50.40 ± 4.30#
AST, IU/l	14.90 ± 3.80	62.80 ± 4.85*	52.40 ± 3.70#	41.20 ± 3.60#	28.40 ± 2.90#

Data presented as mean ± SD ($n = 10$ rats per group).
*$P < 0.05$ versus control group; # $P < 0.05$ versus NAFLD group; one-way analysis of variance followed by Tukey's multiple comparison test.
NAFLD, nonalcoholic fatty liver disease induced by a high-fat diet; ANB-L, low-dose (5 mg/kg/day) arnebin-1 treatment group; ANB-M, medium-dose (10 mg/kg/day) arnebin-1 treatment group; ANB-H, high-dose (20 mg/kg/day) arnebin-1 treatment group; ALT, alanine aminotransferase; AST, aspartate aminotransferase.

HDL-C and LDL-C levels were examined. As shown in Table 2, the serum TC, TG and LDL-C levels in HFD-fed rats (NAFLD group) were higher than those of the control rats ($P < 0.05$ for TG and LDL-C). However, 12 weeks of treatment with arnebin-1 was associated with significantly reduced levels of the above biochemical parameters compared with the NAFLD group ($P < 0.05$ for all comparisons except for TC). Moreover, the level of serum HDL-C in HFD-fed rats (NAFLD group) was significantly lower than in the control rats ($P < 0.05$), and this decrease was dramatically inhibited by 60.5% after arnebin-1 treatment at the dose of 20 mg/kg/day.

The histopathological examination of the liver tissue samples verified the results obtained from the biochemical tests. Results with haematoxylin and eosin staining showed that hepatic lobules had a disordered arrangement combined with fatty degeneration of the hepatocytes in HFD-fed rats (NAFLD group) compared with the control rats. However, these changes were noticeably attenuated by arnebin-1 treatment (Figure 1a). Similarly, arnebin-1 treatment also decreased lipid droplet deposition in hepatocytes induced by HFD as shown by oil red O staining (Figure 1b). Consistent with the changes of serum lipids, the hepatic TC and TG levels were both significantly increased after HFD treatment (NAFLD group) compared with the control group ($P < 0.05$ for both comparisons), while arnebin-1 administration was associated with significantly reduced hepatic TC and TG levels compared with the NAFLD group ($P < 0.05$ for all comparisons) (Figures 1c and 1d).

As presented in Figure 2a, HFD led to an increase in the deposition of collagen fibrils in liver tissues and arnebin-1 treatment reduced the deposition of collagen in a dose-dependent manner. To further confirm the effect of arnebin-1 on liver fibrosis, the study examined several important tissue factors associated with hepatic fibrosis, such as PAI-1, CTGF, collagen III and collagen IV. HFD significantly increased PAI-1, CTGF, collagen III and collagen IV mRNA levels compared with the control group ($P < 0.05$ for all comparisons); and these increases were significantly attenuated after arnebin-1 treatment compared with the NAFLD group ($P < 0.05$ for all comparisons) (Figures 2b–2e).

Table 2. Serum lipid profiles in control and experimental groups of Sprague–Dawley rats after 10 weeks of either a standard diet (control group) or a high-fat diet followed by 12 weeks of treatment with either saline (NAFLD group) or arnebin-1 in addition to the existing diet.

	Groups of Sprague–Dawley rats				
Parameters	Control	NAFLD	ANB-L	ANB-M	ANB-H
TC, mmol/l	1.31 ± 0.14	2.73 ± 0.24	2.34 ± 0.18	2.01 ± 0.13	1.67 ± 0.15
TG, mmol/l	0.91 ± 0.04	1.63 ± 0.14*	$1.34 \pm 0.09^{\#}$	$1.21 \pm 0.08^{\#}$	$1.11 \pm 0.07^{\#}$
HDL-C, mmol/l	1.11 ± 0.09	0.73 ± 0.06*	$0.84 \pm 0.07^{\#}$	$0.91 \pm 0.06^{\#}$	$0.96 \pm 0.06^{\#}$
LDL-C, mmol/l	0.53 ± 0.04	0.78 ± 0.07*	$0.71 \pm 0.06^{\#}$	$0.66 \pm 0.05^{\#}$	$0.61 \pm 0.04^{\#}$

Data presented as mean $\pm$ SD ($n = 10$ rats per group).

*$P < 0.05$ versus control group; $^{\#}P < 0.05$ versus NAFLD group; one-way analysis of variance followed by Tukey's multiple comparison test.

NAFLD, nonalcoholic fatty liver disease induced by a high-fat diet; ANB-L, low-dose (5 mg/kg/day) arnebin-1 treatment group; ANB-M, medium-dose (10 mg/kg/day) arnebin-1 treatment group; ANB-H, high-dose (20 mg/kg/day) arnebin-1 treatment group; TC, total cholesterol; TG, triglycerides; HDL-C, high-density lipoprotein cholesterol; LDL-C, low-density lipoprotein cholesterol.

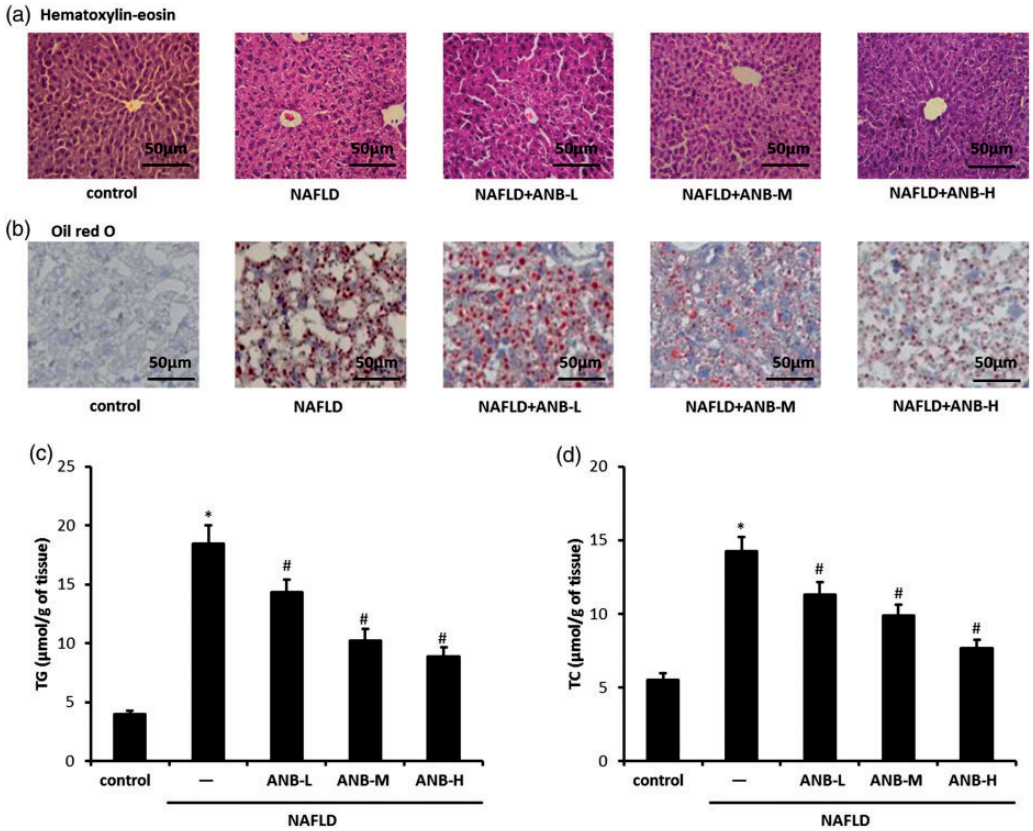

Figure 1. Effect of arnebin-1 on high-fat diet (HFD)-induced liver injury and lipid accumulation. (a and b) Nonalcoholic fatty liver disease (NAFLD) was induced by feeding Sprague–Dawley rats for 22 weeks with HFD. After feeding HFD for 10 weeks, the rats were administrated low, medium or high doses (5 mg/kg/day, 10 mg/kg/day or 20 mg/kg/day, respectively) of arnebin-1 (ANB-L, ANB-M, ANB-H, respectively) for the last 12 weeks of a total of 22 weeks of HFD. Haematoxylin and eosin staining (a) and oil red O staining (b) of liver sections. Scale bar 50 μm. Triglycerides (TG; c) and total cholesterol (TC; d) levels in liver tissues after HFD with or without treatment with different doses of arnebin-1. Data are presented as mean ± SD. $^{*}P < 0.05$ versus the control group; $^{\#}P < 0.05$ versus the NAFLD group, $n = 6$ rats per group; one-way analysis of variance followed by Tukey's multiple comparison test. The colour version of this figure is available at: http://imr.sagepub.com.

To elucidate the potential mechanism by which arnebin-1 attenuated lipid accumulation and liver fibrosis during NAFLD, the levels of PPARγ, MMP-9 and TIMP-1 proteins were examined using Western blot analyses, which demonstrated that the HFD insult significantly decreased the protein levels of PPARγ and pro-MMP-9 compared with the control group ($P < 0.05$ for all comparisons), while it significantly increased the levels of TIMP-1 compared with the control group ($P < 0.05$). The above changes of protein levels were all significantly attenuated after arnebin-1 treatment compared with the NAFLD group ($P < 0.05$ for all comparisons) (Figures 3a–3c). Consistent with the results of the Western blotting, arnebin-1 treatment inhibited the decrease of PPARγ and MMP-9 mRNA levels and the increase of

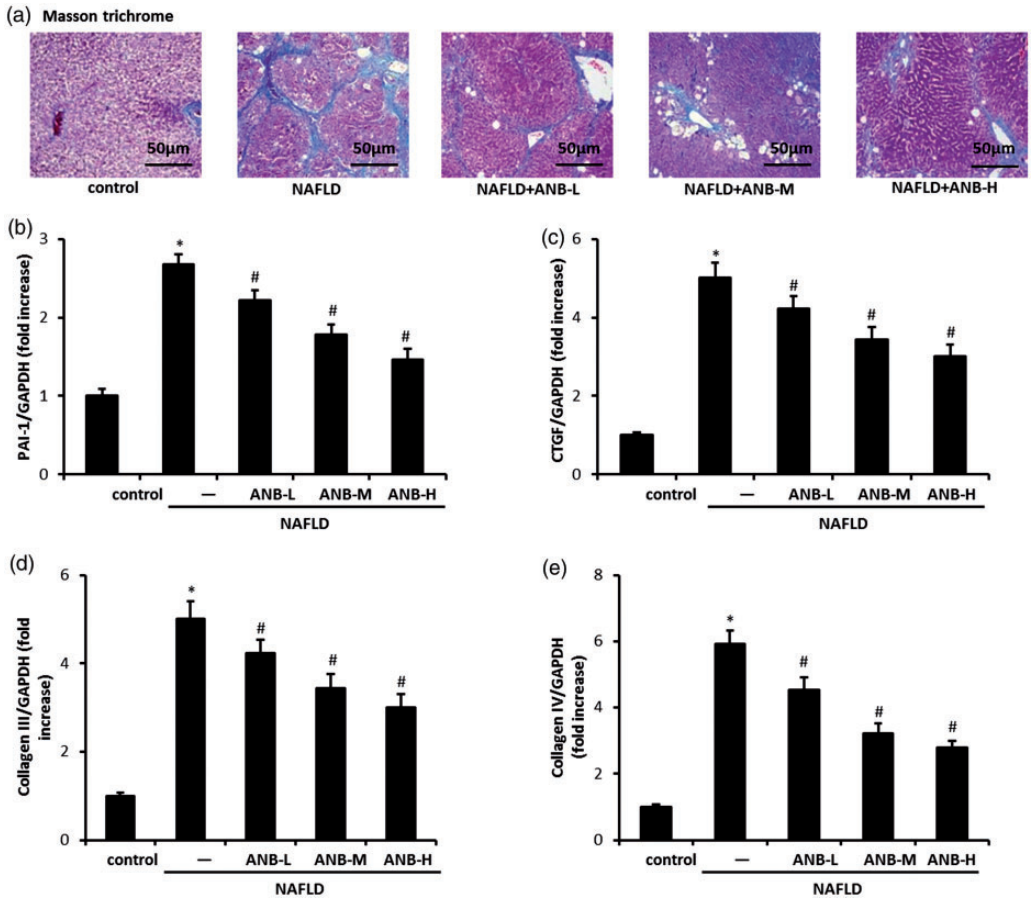

Figure 2. Effect of arnebin-1 on high-fat diet (HFD)-induced liver fibrosis. (a) Masson trichrome staining of liver sections. Representative images of liver tissues isolated from the control group, nonalcoholic fatty liver disease (NAFLD) group, ANB-L group (5 mg/kg/day arnebin-1), ANB-M group (10 mg/kg/day arnebin-1) and ANB-H group (20 mg/kg/day arnebin-1). Scale bar 50 μm. (b–e) Quantitative polymerase chain reaction showed increased plasminogen activator inhibitor type 1 (PAI-1) (b), connective tissue growth factor (CTGF) (c), collagen III (d) and collagen IV (e) mRNA levels in liver tissues from HFD-induced NAFLD rats, which were inhibited after treatment with arnebin-1. Data are presented as mean ± SD. $^{*}P < 0.05$ versus the control group; $^{\#}P < 0.05$ versus the NAFLD group, $n = 8$ rats per group; one-way analysis of variance followed by Tukey's multiple comparison test. The colour version of this figure is available at: http://imr.sagepub.com.

TIMP-1 mRNA levels (data not shown). Similarly, ELISAs revealed that HFD administration significantly decreased the concentration of MMP-9 and significantly increased the concentration of TIMP-1 in serum and liver tissues compared with the control group ($P < 0.05$ for all comparisons), which was ameliorated by arnebin-1 treatment compared with the NAFLD group ($P < 0.05$ for all comparisons) (Figures 3d–3g). The gelatinolytic activity of MMP-9 was then determined because Western blotting or ELISAs may determine the levels of both activated and inactivated forms of MMP-9. The results showed that arnebin-1 treatment reversed the

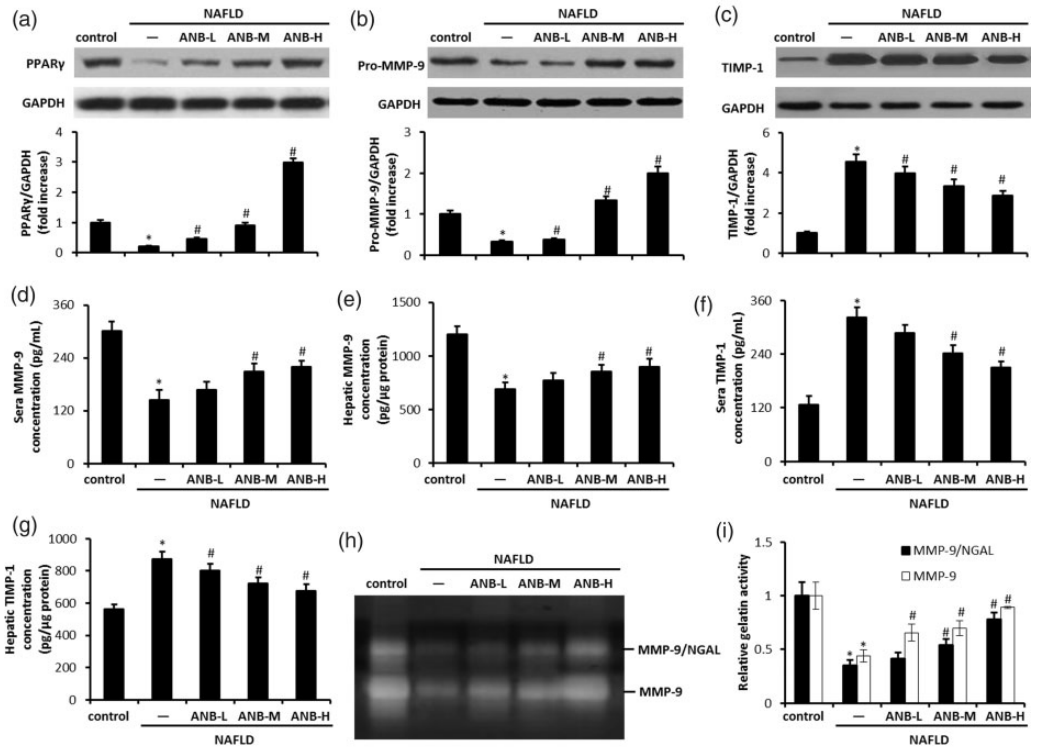

Figure 3. Effects of arnebin-1 on hepatic proliferator-activated receptor γ (PPARγ), matrix-metalloproteinase-9 (MMP-9) and tissue inhibitor of metalloproteinase-1 (TIMP-1) protein levels in the control group, nonalcoholic fatty liver disease (NAFLD) group, ANB-L group (5 mg/kg/day arnebin-1), ANB-M group (10 mg/kg/day arnebin-1) and ANB-H group (20 mg/kg/day arnebin-1). (a–c) The livers were isolated at the end of the experimental period. The levels of PPARγ (a), pro-MMP-9 (b) and TIMP-1 (c) proteins in livers were determined using Western blot analyses. Densitometric analysis showed that arnebin-1 inhibited the decrease of PPARγ and MMP-9 protein levels and the increase of TIMP-1 levels that were induced by the high-fat diet (NAFLD group). (d–g) The concentration of MMP-9 (d and e) and TIMP-1 (f and d) in serum and liver tissues, respectively, were determined using enzyme-linked immunosorbent assays. (h) The gelatinolytic activities of MMP-9 and MMP-9/neutrophil gelatinase-associated lipocalin (NGAL) complex were detected in the zymogram incubation buffer. (i) Quantification of MMP-9 and MMP-9/NGAL activities in gelatin gels. Data are presented as mean ± SD. $^{*}P < 0.05$ versus control group; $^{\#}P < 0.05$ versus NAFLD group, $n = 6$ rats per group; one-way analysis of variance followed by Tukey's multiple comparison test.

HFD-induced decrease of MMP-9 gelatinolytic activity in liver tissues (Figures 3h and 3i). HFD also significantly reduced the gelatinolytic activity of MMP-9/NGAL complex, which is critical for the maintenance of the enzymatic activity of MMP-9,[17] compared with the control group ($P < 0.05$); while this decrease was attenuated by arnebin-1 treatment.

Insulin resistance (IR) is also a typical clinical symptom of NAFLD.[2,6,18] HFD significantly increased fasting blood glucose and insulin levels compared with the control group ($P < 0.05$ for all comparisons), which were ameliorated by arnebin-1 treatment compared with the NAFLD group ($P < 0.05$ for all comparisons) (Figures 4a and 4b). Moreover, HOMA-IR index

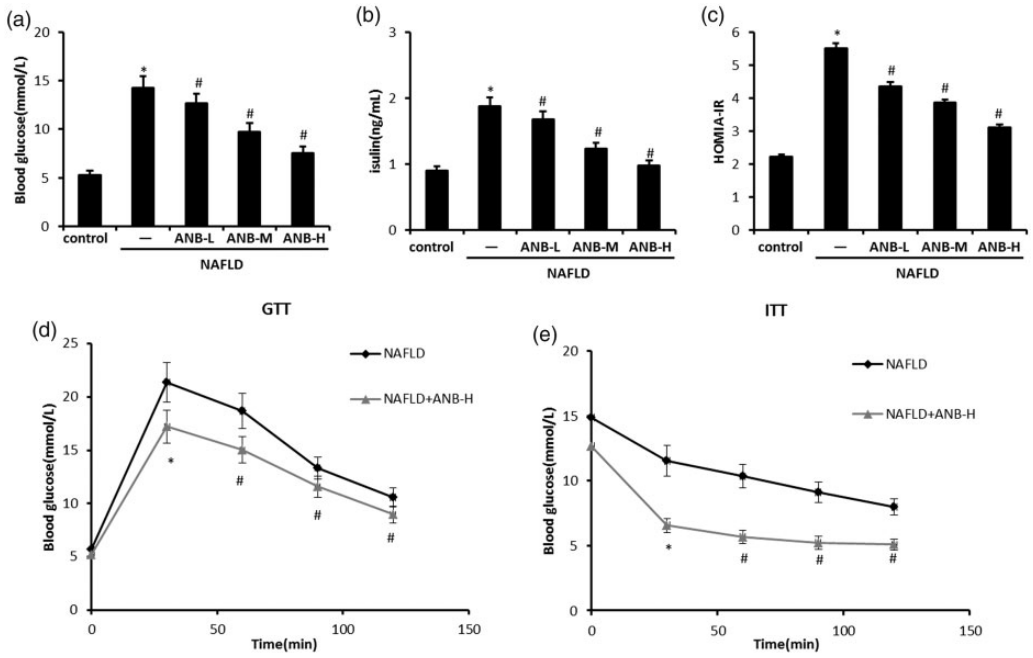

Figure 4. Effects of arnebin-1 on blood glucose levels and insulin resistance in the control group, nonalcoholic fatty liver disease (NAFLD) group, ANB-L group (5 mg/kg/day arnebin-1), ANB-M group (10 mg/kg/day arnebin-1) and ANB-H group (20 mg/kg/day arnebin-1). Arnebin-1 attenuated high-fat diet (HFD)-induced insulin resistance. Plasma fasting glucose (a), insulin (b) and homeostasis model assessment of IR (HOMA-IR) values (c) were measured at the end of experiment. Glucose tolerance test (GTT) (d) and insulin tolerance test (ITT) (e) in HFD-fed rats with or without arnebin-1 treatment. Data are presented as mean ± SD. *$P < 0.05$ versus the control group; $^{\#}P < 0.05$ versus the NAFLD group, $n = 8$ rats per group; one-way analysis of variance followed by Tukey's multiple comparison test.

indicated that systemic IR was decreased after arnebin-1 administration (Figure 4c). The GTT and ITT showed that arnebin-1 treatment could efficiently clear plasma glucose after either a glucose or insulin intraperitoneal injection (Figures 4d and 4e).

To understand how arnebin-1 prevents IR, the study determined the effects of arnebin-1 on insulin signalling. As shown in Figures 5a–5d, in HFD-treated rats, arnebin-1 treatment increased IRS-1 phosphorylation at Tyr608, Akt phosphorylation at Ser473 and mTOR phosphorylation at Ser2448 and inhibited IRS-1 phosphorylation at Ser307 in the presence of an insulin injection. Moreover, arnebin-1 treatment further potentiated insulin injection-induced activation of insulin signalling. To support the *in vivo* findings reported above, human HepG2 cells were incubated with arnbin-1 followed by insulin treatment for different time-points as indicated. In HepG2 cells, insulin treatment also led to increased phosphorylation of IRS-1 (Tyr612), Akt (Ser473) and mTOR (Ser2448) (Figures 5e–5g).

Discussion

The present study investigated the effects of arnebin-1 on HFD-induced NAFLD in rats. The HFD model has been widely used to induce NAFLD in multiple studies.[2,19] Therefore, here, a rat model of NAFLD was induced by feeding an HFD

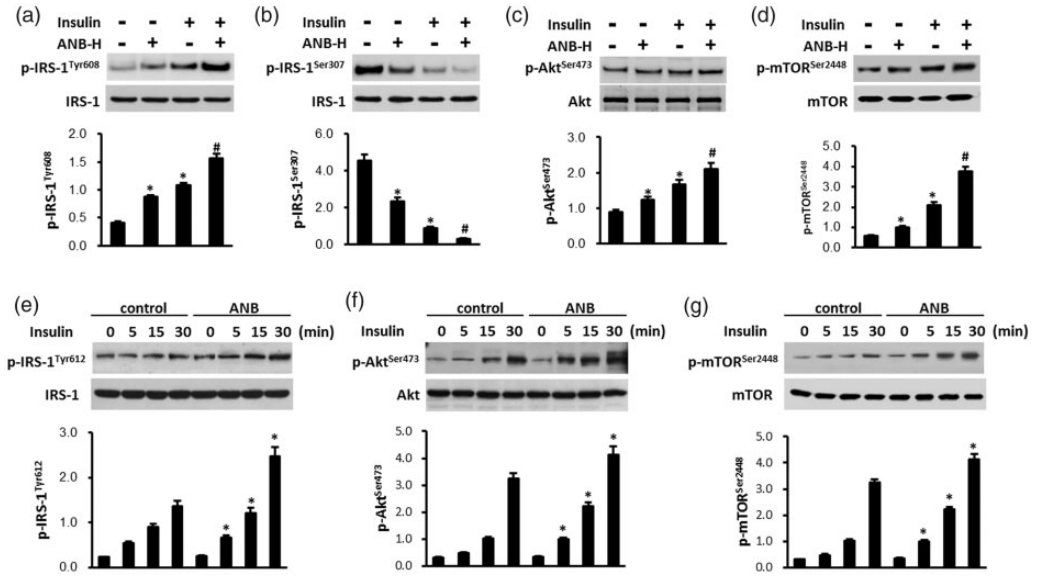

Figure 5. Effects of arnebin-1 on the hepatic insulin signalling pathway. Phosphorylation of insulin receptor substrate (IRS)-1 (Tyr608) (a), IRS-1 (Ser307) (b), Akt (Ser473) (c) and mTOR (Ser2448) (d) in the livers of high-fat diet (HFD)-fed rats before or after arnebin-1 treatment for 12 weeks (a total of 22 weeks of an HFD) in response to an intraperitoneal injection of insulin (1.0 IU/kg for 15 min) as determined by Western blot analyses. Data are presented as mean ± SD. $^{*}P < 0.05$ versus the NAFLD group; $^{\#}P < 0.05$ versus the NAFLD+insulin group, $n = 8$ rats per group; one-way analysis of variance followed by Tukey's multiple comparison test. HepG2 cells were treated with arnebin-1 (10 μg/ml) for 48 h prior to insulin (100 μmol/l) for different time-points as indicated. Phosphorylation of IRS-1 (Tyr612) (e), Akt (Ser473) (f) and mTOR (Ser2448) (g) were determined by Western blot analyses. Data are presented as mean ± SD. $^{*}P < 0.05$ versus corresponding time-point (0 h) in the control group or arnebin-1-treated group; one-way analysis of variance followed by Tukey's multiple comparison test.

for 22 weeks. HFD induced significant weight gain in the NAFLD group and this increase was significantly attenuated by arnebin-1 in a dose-dependent manner. In addition to the weight gain, abnormal serum biochemical parameters and dyslipidaemia were observed in HFD-fed rats, which were attenuated by arnebin-1 treatment. Additionally, HFD led to a higher level of serum ALT and AST, which was indicative of hepatocyte injury. However, the increased levels of serum ALT and AST were alleviated in response to all doses of arnebin-1. Furthermore, the hepatic injury was also attenuated by arnebin-1 treatment, as suggested by reduced hepatocyte ballooning, inflammatory cell infiltration, lipid accumulation and hepatic TG and TC levels. Collectively, this study demonstrates for the first time that arnebin-1 can improve hepatic lipid accumulation and injury induced by HFD.

In addition to inhibition of lipid accumulation, this current study also found that arnebin-1 could alleviate HFD-induced liver fibrosis. Lower deposition of collagen fibrils in liver was observed in arnebin-1-treated HFD-fed rats. PAI-1 is an inhibitor of extracellular matrix (ECM)-degrading enzymes, which play an important role in regulating fibrinolysis. Upregulation of PAI-1 levels inhibits the activity of the fibrinolytic system and MMPs, thus further accelerates the progression of liver fibrosis.[20]

Meanwhile, CTGF overexpression is associated with increased ECM protein levels such as collagen III and collagen IV.[21] In this current study, HFD-induced increases of the levels of PAI-1 and CTGF were ameliorated after arnebin-1 treatment. As expected, the increased levels of type III and IV collagen were also reduced by arnebin-1 administration.

Proliferator-activated receptor γ is suggested to play an important role in regulating lipid storage and differentiation in adipocytes and macrophages.[22] Previous studies have indicated that PPARγ is related to the control of insulin resistance, lipid metabolism and inflammation in liver steatosis.[1,5] The agonists of PPARγ can enhance insulin sensitivity and lipid accumulation in adipose, liver and skeletal muscle tissues.[23,24] It has been found that hepatic PPARγ protein levels and mRNA expression were decreased in insulin resistance accompanied by the development of NAFLD in HFD-fed rats.[25] Consistent with those findings, this current study also found lower levels of PPARγ in the NAFLD group than in the control group. However, the decreased PPARγ levels were restored after arnebin-1 treatment, indicating the restoration of PPARγ levels may at least partially underly the inhibitory effect of arnebin-1 on hepatic lipid accumulation.

Matrix-metalloproteinases are closely associated with the metabolism of collagen and ECM degradation.[1,26] Several MMPs have been suggested to be expressed in human liver, such as MMP-1, MMP-9, MMP-10 and MMP-11.[27,28] The activity of MMPs is regulated through the action of specific inhibitors, including TIMPs. Increased levels of TIMP-1 can be observed in experimental rats with liver fibrosis.[29] The degree of collagen deposition and fibrosis is critically regulated by the balance between MMPs and TIMPs.[30] In this current study, pro-MMP-9 levels were decreased and TIMP-1 levels were increased in the livers of HFD-fed NAFLD rats. These results were consistent with the report that TIMP-1 expression was inhibited in the CCl_4-induced rat hepatic fibrosis model.[30] However, higher pro-MMP-9 levels were found in the arnebin-1 treatment groups than in the NAFLD group. Moreover, HFD-induced TIMP-1 expression was significantly downregulated after arnebin-1 treatment. The current study also confirmed by using ELISAs that arnebin-1 treatment inhibited the HFD-induced decrease of MMP-9 concentration and the increase of TIMP-1 concentration in serum and liver tissues. It is likely that the concentration of MMP-9 is inversely correlated with TIMP-1. Notably, the antibody included in the ELISA kits or Western blotting procedures might bind to both the activated and inactivated forms of MMP-9. Thus, the gelatinolytic activity of MMP-9 was examined by zymography. Similar to the results of the Western blots and ELISAs, the decreased MMP-9 gelatinolytic activity in liver tissues induced by HFD was reversed by arnebin-1. NGAL is a glycoprotein that binds to MMP-9, which in turn increases the enzymatic activity of MMP-9 by protecting it from proteolytic degradation.[17] The present data demonstrated that arnebin-1 restored the decreased gelatinolytic activity of MMP-9/NGAL induced by HFD. Collectively, these results suggest that arnebin-1 attenuates HFD-induced liver fibrosis by regulating the balance between MMP-9 and TIMP-1.

This current study also demonstrated that arnebin-1 treatment could limit glucose intolerance and IR. Insulin plays an important role in the regulation of hepatic glycogen synthesis and glucose homeostasis via IRS-1, which is responsible for the transduction of insulin signaling.[31] When insulin binds to the insulin receptor, IRS-1 is activated by phosphorylation at Tyr608/612, leading to activation of the insulin signalling

pathway.[31,32] In contrast, insulin signalling is inhibited by IRS-1 phosphorylation at Ser307, resulting in glucose intolerance and IR.[33] Furthermore, phosphorylation of IRS-1 downstream Akt (Ser473) signalling causes mTOR activation by phosphorylation at Ser2448.[18] Importantly, research has demonstrated the dysregulation of the Akt/mTOR signalling pathway in NAFLD.[32,34] In this current study, arnebin-1 treatment promoted insulin injection-induced IRS-1 (Tyr608) phosphorylation and IRS-1 (Ser307) dephosphorylation. Moreover, the activation of the IRS-1/Akt/mTOR signalling pathway induced by insulin was also potentiated by arnebin-1 treatment. Similar results were also observed in human HepG2 cells, in which arnebin-1 enhanced insulin-induced IRS-1/Akt/mTOR signalling activation.

In conclusion, these current data demonstrate that arnebin-1 can partially ameliorate HFD-induced lipid accumulation, liver injury, hepatic fibrosis and IR. These findings indicate that arnebin-1 may be a potential therapeutic agent for NAFLD treatment.

Declaration of conflicting interest

The authors declare that there are no conflicts of interest.

Funding

This work was supported by the National Natural Science Foundation of China (no. 81804163) and Zhejiang Science and Technology Programme of Traditional Chinese Medicine (no. 2012ZQ002).

References

1. Lutchman G, Modi A, Kleiner DE, et al. The effects of discontinuing pioglitazone in patients with nonalcoholic steatohepatitis. *Hepatology* 2007; 46: 424–429.
2. Angulo P. Nonalcoholic fatty liver disease. *N Engl J Med* 2002; 346: 1221–1231.
3. Poloz Y and Stambolic V. Obesity and cancer, a case for insulin signaling. *Cell Death Dis* 2015; 6: e2037.
4. Day CP and James OF. Steatohepatitis: a tale of two "hits"? *Gastroenterology* 1998; 114: 842–845.
5. Nan YM, Fu N, Wu WJ, et al. Rosiglitazone prevents nutritional fibrosis and steatohepatitis in mice. *Scand J Gastroenterol* 2009; 44: 358–365.
6. Piacentini M, Baiocchini A, Del Nonno F, et al. Non-alcoholic fatty liver disease severity is modulated by transglutaminase type 2. *Cell Death Dis* 2018; 9: 257.
7. Harrison SA and Day CP. Benefits of lifestyle modification in NAFLD. *Gut* 2007; 56: 1760–1769.
8. Vilar-Gomez E, Martinez-Perez Y, Calzadilla-Bertot L, et al. Weight loss through lifestyle modification significantly reduces features of nonalcoholic steatohepatitis. *Gastroenterology* 2015; 149: 367–378.
9. Chen X, Yang L, Oppenheim JJ, et al. Cellular pharmacology studies of shikonin derivatives. *Phytother Res* 2002; 16: 199–209.
10. Kim GW, Lin JE, Blomain ES, et al. Antiobesity pharmacotherapy: new drugs and emerging targets. *Clin Pharmacol Ther* 2014; 95: 53–66.
11. Pandeti S, Arha D, Mishra A, et al. Glucose uptake stimulatory potential and antidiabetic activity of the Arnebin-1 from Arnabia nobelis. *Eur J Pharmacol* 2016; 789: 449–457.
12. Zeng Z and Zhu BH. Arnebin-1 promotes the angiogenesis of human umbilical vein endothelial cells and accelerates the wound healing process in diabetic rats. *J Ethnopharmacol* 2014; 154: 653–662.
13. Su ML, He Y, Li QS, et al. Efficacy of acetylshikonin in preventing obesity and hepatic steatosis in db/db mice. *Molecules* 2016; 21: E976.
14. Su M, Huang W and Zhu B. Acetylshikonin from zicao prevents obesity in rats on a high-fat diet by inhibiting lipid accumulation and inducing lipolysis. *PLoS One* 2016; 11: e0146884.
15. Schneider CA, Rasband WS and Eliceiri KW. NIH Image to ImageJ: 25 years of

image analysis. *Nat Methods* 2012; 9: 671–675.
16. Ranjbaran J, Farimani M, Tavilani H, et al. Matrix metalloproteinases 2 and 9 and MMP9/NGAL complex activity in women with PCOS. *Reproduction* 2016; 151: 305–311.
17. Bolignano D, Donato V, Lacquaniti A, et al. Neutrophil gelatinase-associated lipocalin (NGAL) in human neoplasias: a new protein enters the scene. *Cancer Lett* 2010; 288: 10–16.
18. Czech MP. Insulin action and resistance in obesity and type 2 diabetes. *Nat Med* 2017; 23: 804–814.
19. Kucera O and Cervinkova Z. Experimental models of non-alcoholic fatty liver disease in rats. *World J Gastroenterol* 2014; 20: 8364–8376.
20. McMahon EG. Recent studies with eplerenone, a novel selective aldosterone receptor antagonist. *Curr Opin Pharmacol* 2001; 1: 190–196.
21. Weston BS, Wahab NA and Mason RM. CTGF mediates TGF-beta-induced fibronectin matrix deposition by upregulating active alpha5beta1 integrin in human mesangial cells. *J Am Soc Nephrol* 2003; 14: 601–610.
22. Law RE, Goetze S, Xi XP, et al. Expression and function of PPARgamma in rat and human vascular smooth muscle cells. *Circulation* 2000; 101: 1311–1318.
23. Mohammadi A, Gholamhoseinian A and Fallah H. Zataria multiflora increases insulin sensitivity and PPARgamma gene expression in high fructose fed insulin resistant rats. *Iran J Basic Med Sci* 2014; 17: 263–270.
24. Rani S and O'Driscoll L. Analysis of changes in phosphorylation of receptor tyrosine kinases: antibody arrays. *Methods Mol Biol* 2015; 1233: 15–23.
25. Zhao W, Liu L, Wang Y, et al. Effects of a combination of puerarin, baicalin and berberine on the expression of proliferator-activated receptor-γ and insulin receptor in a rat model of nonalcoholic fatty liver disease. *Exp Ther Med* 2016; 11: 183–190.
26. Hemmann S, Graf J, Roderfeld M, et al. Expression of MMPs and TIMPs in liver fibrosis – a systematic review with special emphasis on anti-fibrotic strategies. *J Hepatol* 2007; 46: 955–975.
27. Lichtinghagen R, Bahr MJ, Wehmeier M, et al. Expression and coordinated regulation of matrix metalloproteinases in chronic hepatitis C and hepatitis C virus-induced liver cirrhosis. *Clin Sci (Lond)* 2003; 105: 373–382.
28. Garciade Leon Mdel C, Montfort I, Tello Montes E, et al. Hepatocyte production of modulators of extracellular liver matrix in normal and cirrhotic rat liver. *Exp Mol Pathol* 2006; 80: 97–108.
29. Xu GF, Li PT, Wang XY, et al. Dynamic changes in the expression of matrix metalloproteinases and their inhibitors, TIMPs, during hepatic fibrosis induced by alcohol in rats. *World J Gastroenterol* 2004; 10: 3621–3627.
30. Xie SR, An JY, Zheng LB, et al. Effects and mechanism of adenovirus-mediated phosphatase and tension homologue deleted on chromosome ten gene on collagen deposition in rat liver fibrosis. *World J Gastroenterol* 2017; 23: 5904–5912.
31. Kumashiro N, Erion DM, Zhang D, et al. Cellular mechanism of insulin resistance in nonalcoholic fatty liver disease. *Proc Natl Acad Sci U S A* 2011; 108: 16381–16385.
32. Taniguchi CM, Ueki K and Kahn CR. Complementary roles of IRS-1 and IRS-2 in the hepatic regulation of metabolism. *J Clin Invest* 2016; 126: 4387.
33. Thirone AC, Huang C and Klip A. Tissue-specific roles of IRS proteins in insulin signaling and glucose transport. *Trends Endocrinol Metab* 2006; 17: 72–78.
34. Hwang HJ, Jung TW, Kim BH, et al. A dipeptidyl peptidase-IV inhibitor improves hepatic steatosis and insulin resistance by AMPK-dependent and JNK-dependent inhibition of LECT2 expression. *Biochem Pharmacol* 2015; 98: 157–166.